CFD Simulation of a Heated Round Jet of Sodium in Forced Flow Regime (TEFLU Benchmark)

C. Aragonese, S. Buono, G. Fotia, L. Maciocco, V. Moreau, L. Sorrentino

17 November 2000

Abstract

The results of the simulation of the forced-flow case of the TEFLU benchmark [1], obtained at CRS4 with the Star-CD code, are reported.

First, a comparison among different k-ε turbulence models implemented in Star-CD was carried out. The Chen k-ε model [4], [5] gave the best agreement with experimental results.

Then, a study of the influence of the turbulent Prandtl number Pr_t was carried out. The first step was the comparison between the molecular conductivity and the turbulent heat diffusion coefficients, calculated using the turbulent Prandtl number approach (Reynolds analogy). It was found that that the two contributions are of the same order of magnitude. This result implies that there is a strong interaction between the molecular and turbulent heat transfer, which could have a strong effect on the scaling coefficient between the turbulent transfer of momentum and heat, namely on Pr_t.

In order to study the effect of the variation of Pr_t on the temperature profiles, the inlet turbulence kinetic energy profile was scaled in order to obtain a good agreement between calculated and experimental velocity profiles. Then, the value of Pr_t was changed from the standard value of 0.9 to 10 (on the basis of the considerations of Jisha and Rieche [6]) and to 10^4 (to exclude the contribution of the turbulent heat transfer). A very good agreement with experimental measurements was found in both cases (the best being the case of no turbulent heat transfer).

The above results indicate that the heat conduction is predominant in the forced-flow case. In this situation, the standard value 0.9 of Pr_t yields an overestimation of the thermal diffusion rate.

Contents

1 Calculation set-up 2
2 Boundary conditions 3
3 Calculation with the Chen k-ε and comparison with other k-ε models implemented in Star-CD 4
4 Analysis of the influence of the value of the turbulent Prandtl number. 6
5 Conclusions 11
6 References 12

1 Calculation set-up

The sketch of the TEFLU benchmark is shown in Figure 1; the main parameters of the forced-flow case are listed in Table 1. See [1] for a complete description of the TEFLU benchmark.

A non-uniform computational mesh of 70 × 480 cells was used, which guarantees the grid-independence of the solution [1]. A QUICK third-order convection scheme was used for the momentum and energy equations, while an UPWIND first-order scheme was used for the discretisation of the turbulence equations. Boundary conditions are discussed in next section.

The calculations presented in this report are listed in Table 2.

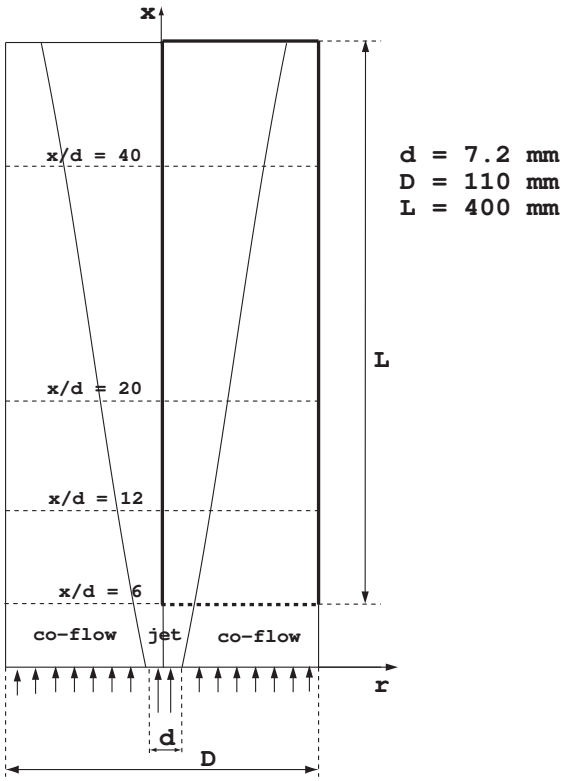

Figure 1: sketch of the TEFLU test case. The calculation domain is traced with thick lines.

Experiment	$\bar{u}_{cf}$ (m/s)	T_{cf} (K)	Re_{cf}	$\Delta\bar{u}_j$ (m/s)	ΔT_j (K)	ρ_j (Kg/m^3)	Re_j	Fr_j	$\dot{m}_{tot}$ (Kg/s)
a) forced jet	0.05	573	1.4×10^4	0.50	30	872.87	1.01×10^4	521	0.436

Table 1: experimental conditions.

	Turbulence model	Inlet k profile	Inlet ε profile	Pr_t
A0	Chen k-ε	not scaled	imposed	0.9
A1	Chen k-ε	not scaled	extrapolated	0.9
A2	Standard k-ε	not scaled	extrapolated	0.9
A3	RNG k-ε	not scaled	extrapolated	0.9
A4	Quadratic k-ε	not scaled	extrapolated	0.9
A5	Cubic k-ε	not scaled	extrapolated	0.9
B1	Chen k-ε	scaled by 0.7	extrapolated	0.9
B2	Chen k-ε	scaled by 0.7	extrapolated	10
B3	Chen k-ε	scaled by 0.7	extrapolated	10^4

Table 2: calculation list

2 Boundary conditions

Boundary conditions are imposed as described in [1]. Concerning the inlet conditions for the turbulence parameters, the following points should be taken into account:

- the inlet profile for the turbulence kinetic energy has been deduced from experiments performed in 1943 [3] on an air jet in stagnant fluid. The jet Reynolds number was 1.4×10^3. Some uncertainties lie in this procedure:
  - the determination of the section corresponding to the TEFLU x/d = 6 section is not straightforward (the decay of the centreline velocity is different in the two cases). Anyway, only measurements in sections at x/d = 5, 10, 15, 20, 30, 40 are reported in the Corrsin paper.
  - Detailed profiles are available only for the axial component of the fluctuation velocity. Some assumptions are necessary for the other two components.
  - The jet Reynolds number is not the same. Being relatively low, it could have an influence on the turbulence levels.
- The inlet profile for the turbulence dissipation has been deduced using a constant mean value of the turbulent viscosity along the inlet section, and scaling the so obtained profile on the basis of numerical experiments.

The alternative option of imposing a zero-order extrapolation condition for ε, proposed in [1], has been tested. This condition implies the assumption of neglecting the inlet fluxes of ε, namely to impose a local equilibrium for the turbulence dissipation. In this case, the inlet ε profile is a result of the calculation.

Figure 2 shows the inlet profiles interpolated on the computational mesh. The two cases of imposed (A0) and extrapolated (A1) ε profile (obtained in case A1) are shown. It can be seen that the extrapolated ε profile is very similar to the imposed one, with slightly higher values. The fact that the resulting profile of turbulent viscosity has its maximum value in the co-flow is considered reasonable, the co-flow Reynolds number being higher (implying a higher turbulence length scale).

As shown in Figure 3, the velocity and temperature axial profiles in the two cases are almost equal. However, it is the author opinion that the extrapolation inlet ε condition is less arbitrary (especially in the cases of buoyant flow), and it has been adopted for all the successive calculations.

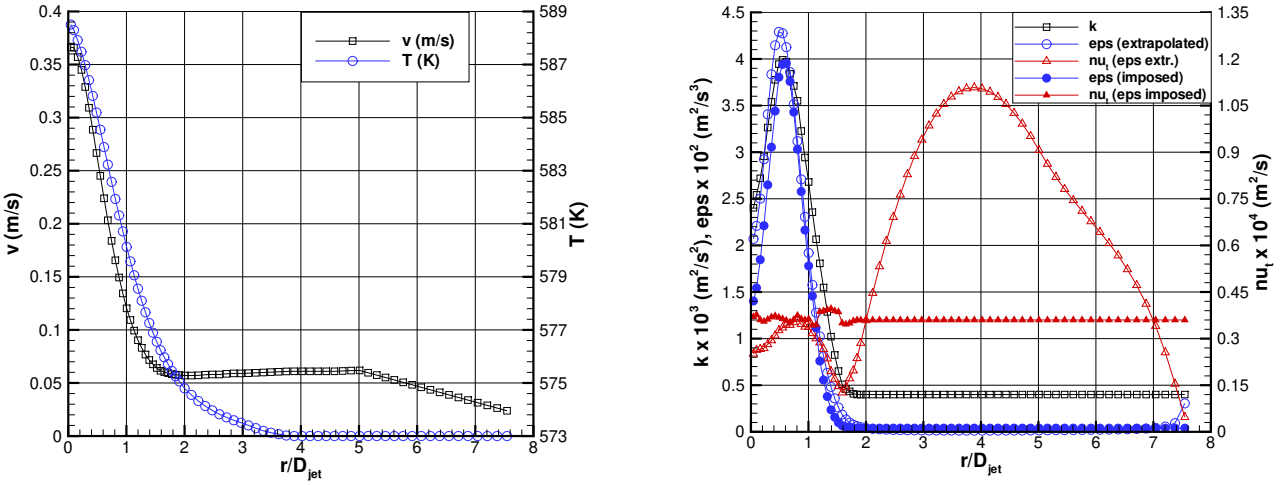

Figure 2: inlet profiles, interpolated on the computational mesh, of velocity (imposed), temperature (imposed), turbulence kinetic energy (imposed), turbulence dissipation (extrapolated for case A1), and turbulent cinematic viscosity (calculated from k and ε profiles).

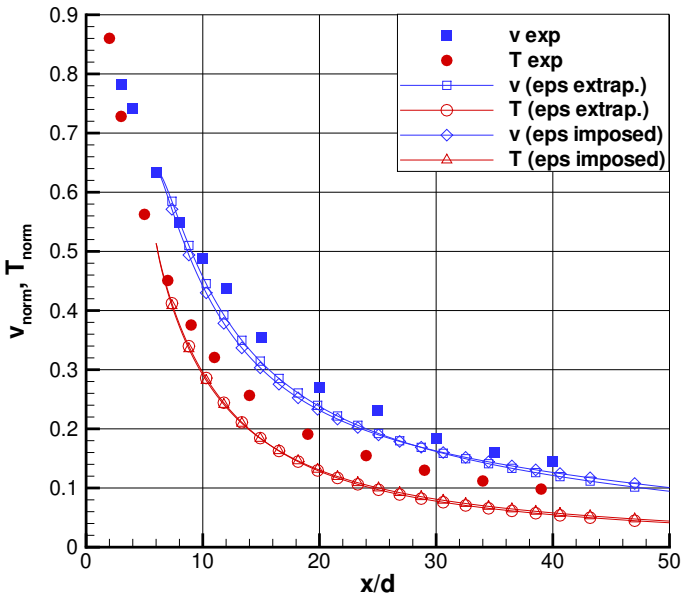

Figure 3: velocity and temperature axial profiles in the two cases of imposed and extrapolated inlet ε profile (cases A0 and A1).

3 Calculation with the Chen k-ε and comparison with other k-ε models implemented in Star-CD

The Chen k-ε [4], [5] has been chosen by the Energy Amplifier group at CRS4 as the reference turbulence model for the calculations related to the preliminary design of the Energy Amplifier

Demonstration Facility. This choice was based on a brief benchmarking analysis of Star-CD capabilities on a set of standard test cases [9]. The peculiarity of this model lies in an extra term in the ε equation introducing an extra time scale of the turbulence production (in the Standard k-ε only the dissipation time scale k/ε is used).

Figure 4 and Figure 5 show the velocity and temperature axial and radial profiles obtained using the Chen k-ε (case A1), compared with experimental measurements. It can be seen that both velocity and temperature jet spreading-rates are under-predicted. The disagreement with experimental measurement is more evident in the case of temperature profiles.

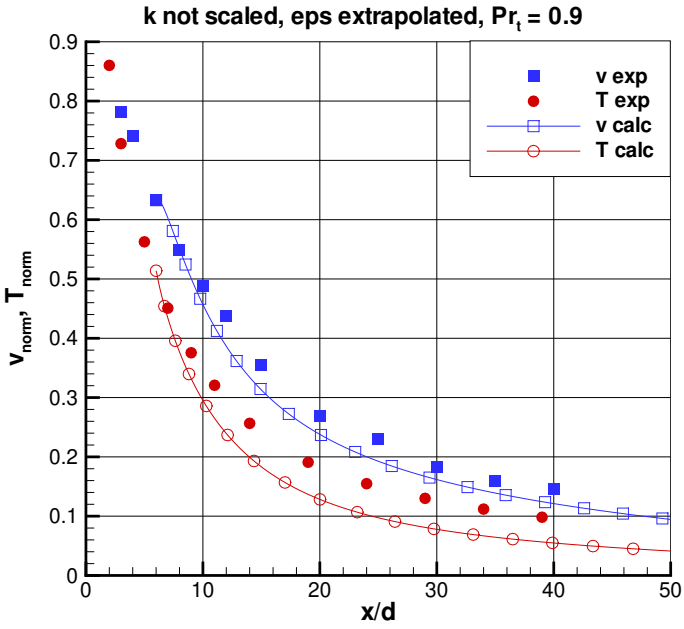

Figure 4: velocity and temperature axial profiles for case A1

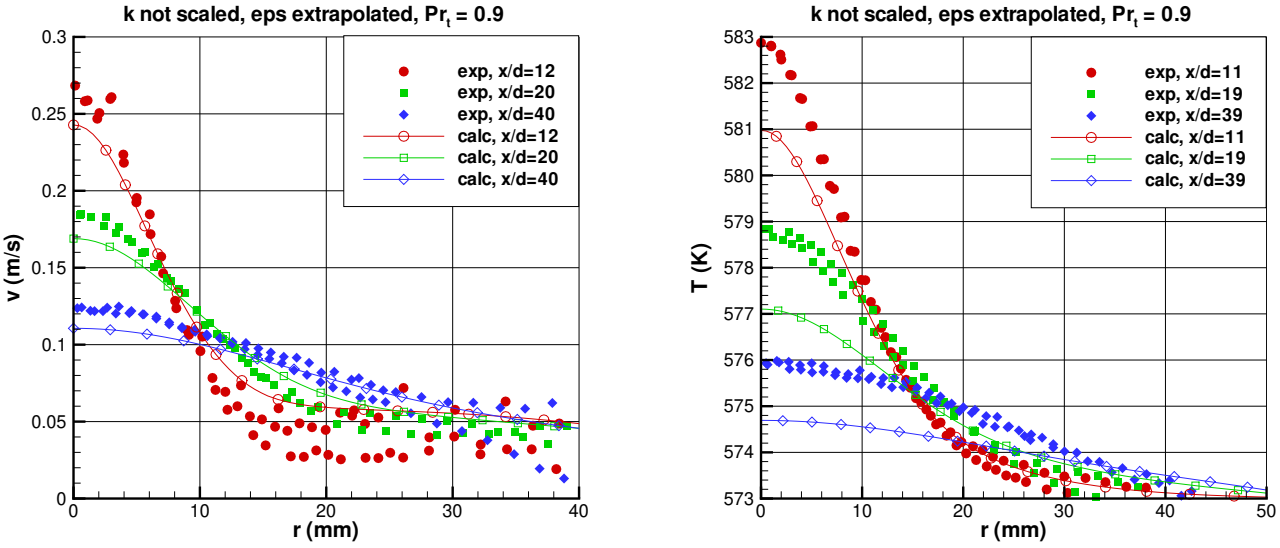

Figure 5: velocity and temperature radial profiles for case A1

The reason of this disagreement could lie either in a bad performance of the turbulence model or in the inlet turbulence conditions. In fact, it is known (see for example [8]) that two-equation turbulence models are not able to correctly reproduce the velocity field of a round jet (round-jet anomaly), yielding an over-prediction of the spreading rate. However, this problem should be reduced by the modification introduced in the dissipation equation of the Chen k-ε model [5]. Moreover, the uncertainties in the inlet conditions could affect significantly the results as well.

The performances of the two-equation turbulence models implemented in Star-CD have been compared (cases A1-A5), in order to get an idea of their problems in simulating a round jet. Figure 6 shows the axial profiles of velocity and temperature. Concerning the velocity spreading-rate, it can be seen as the best results are obtained with the Chen k-ε model, followed by the Standard k-ε model. The RNG k-ε model seems to perform worse than the Standard k-ε model. The Quadratic and Cubic k-ε models, which in theory should reproduce more accurately the Reynolds stress tensor in case of flow anisotropy, give the worse results.

The quality of the prediction of the temperature spreading-rate is nearly the same for the linear models, and slightly worse in the case of the non-linear models. The agreement of the best result with experimental values is worse than in the case of velocity profiles. An explanation to these results will be given in next section.

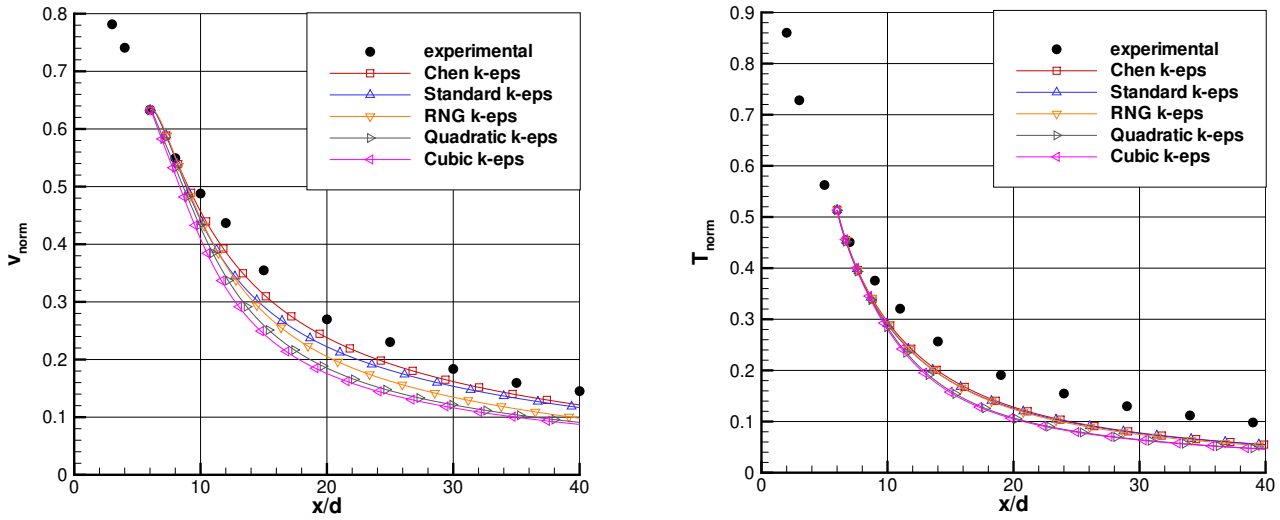

Figure 6: comparison of velocity and temperature axial profiles obtained with different k-ε models implemented in Star-CD (cases A1, A2, A3, A4, A5).

4 Analysis of the influence of the value of the turbulent Prandtl number.

In an incompressible flow where buoyancy effects are not important, the velocity field is uncoupled with the temperature field (apart from the little influence of the variation of the physical properties with temperature). In this case, also the turbulence field (in terms of turbulence energy and turbulence dissipation) is independent of the temperature field. Moreover, in a case like a round jet, where the flow is almost parallel, the main mechanism governing the spreading of temperature is the turbulent diffusion.

If a gradient-diffusion approach is considered applicable, this implies that, given a correct spreading rate for the velocity field, the spreading rate of the thermal field will be correctly reproduced if the turbulent diffusion coefficient

$$\lambda_t = \frac{\nu_t}{Pr_t}$$

is correct, namely, being ν_t correct, if the value of the turbulent Prandtl number is correct.

In order to obtain a velocity field in agreement with experimental results, some calculation were carried out scaling the inlet k profile by a constant (always using the extrapolation condition for ε). Figure 7 and Figure 8 show the results obtained with a scaling factor of 0.7 (axial profiles of case A1 are also reported for comparison). The velocity field is in good agreement with experimental data, while the temperature spreading-rate is still overestimated. This means that the turbulent diffusion coefficient is too high, namely that Pr_t is too low.

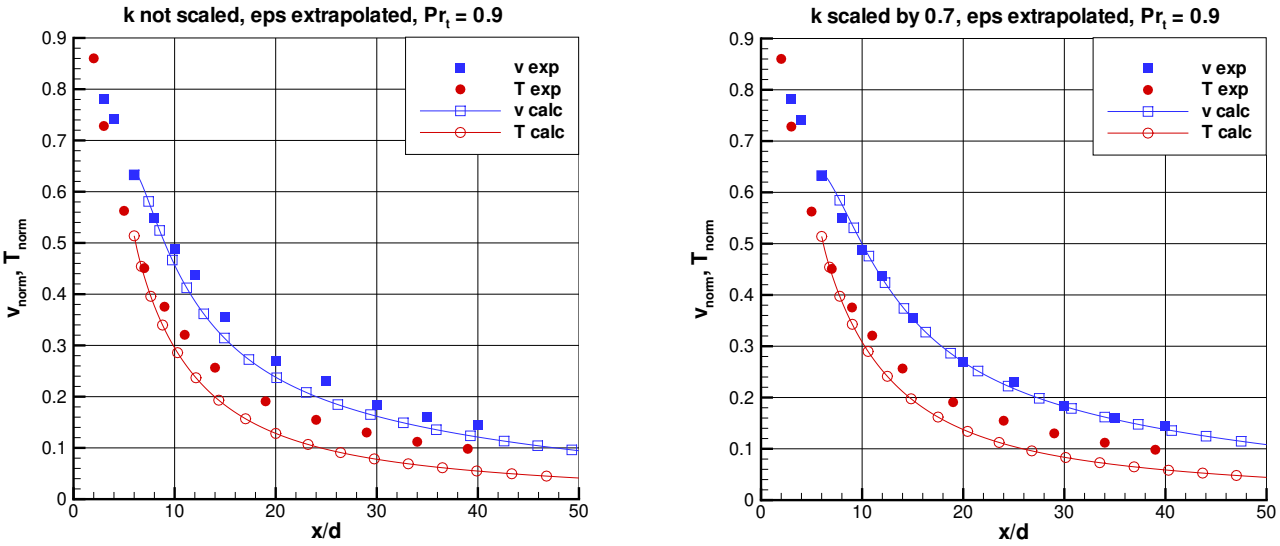

Figure 7: velocity and temperature axial profiles for cases A1 and B1

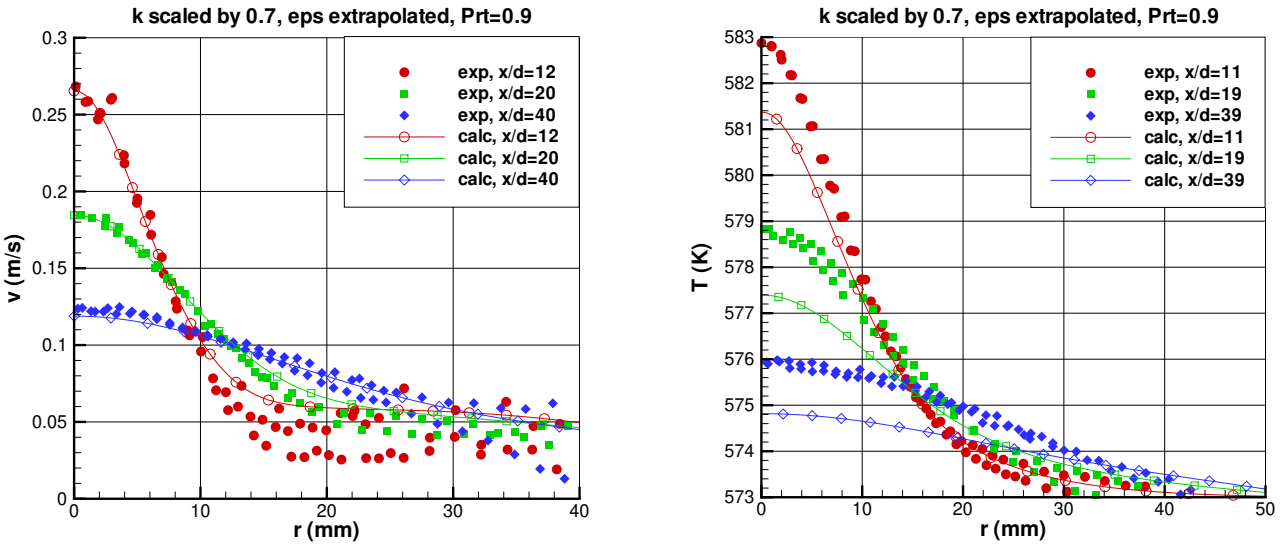

Figure 8: velocity and temperature radial profiles for case B1

This can be explained considering that the Reynolds analogy with a Pr_t of order 1 assumes that the mechanisms of turbulent transport of momentum and energy are the same; this is a reasonable assumption when the contribution of the molecular thermal diffusivity is of minor importance with respect to λ_t.

However, This condition is not verified in our case. Figure 9 shows three radial profiles of the percentage of the turbulent conductivity with respect to the sum of turbulent and the molecular conductivity, namely

$$100\,\frac{K_t}{K+K_t}$$

where K is the thermal conductivity and

$$K_t = \rho C_p \lambda_t = \frac{C_p \mu_t}{Pr_t}.$$

This quantity gives an idea of the relative importance of molecular conduction and turbulent transport of heat. It can be seen that they are of the same order of magnitude. This is due to the combination of the very low Prandtl number of the Sodium and of the relatively low Reynolds number of the jet. In this conditions, a Pr_t of order 1 gives too much importance to the turbulent heat transport and yield to an overestimation of the total (molecular + turbulent) transport coefficient.

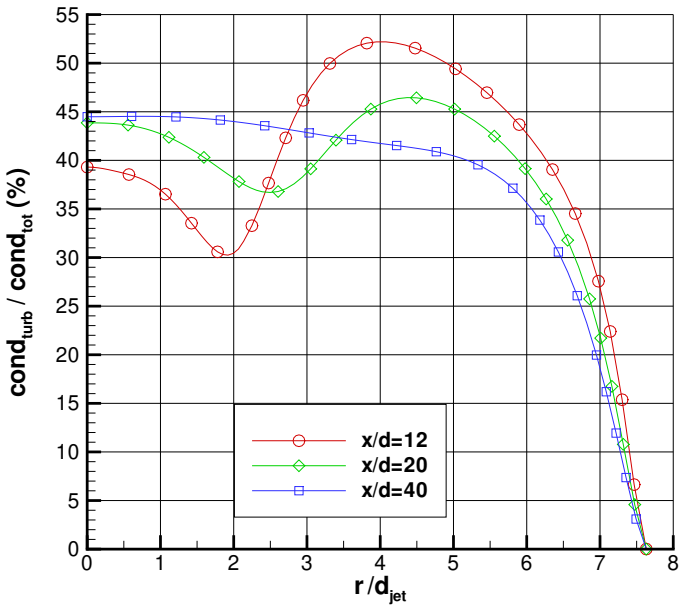

Figure 9: radial profiles of percentage of turbulent heat transport for case B1.

Jisha and Rieke [6], on the basis of theoretical considerations and experimental results, propose the following expression for the turbulent Prandtl number:

$$Pr_t = c_1 + c_2 \frac{1}{Pr\ \ Re^m}$$

$$c_1 = 0.9$$
$$c_2 = 182.4$$
$$m = 0.888$$

In our case we have $Pr = 5.87 \times 10^{-3}$ and $Re = 10^4$, yielding $Pr_t = 9.6$.

Figure 10 and Figure 11 show the results obtained using $Pr_t = 10$ (case B2). The agreement of temperature profiles with experimental measurements is considerably improved. However, a slight overestimation of the temperature spreading-rate can still be observed.

A further calculation was performed with $Pr_t = 10^4$ in order to make the turbulent transport in the energy equation negligible (case B3). As shown in Figure 12 and Figure 13, the best results are obtained in this case. Figure 14 shows the relative importance of turbulent transport in cases B1, B2 and B3.

These results indicate that in the case of the forced-flow regime of the TEFLU benchmark, the only important mechanism for the heat transport is thermal conduction. In this case a turbulent Prandtl number set to 0.9 yields an overestimation of the turbulent heat transport.

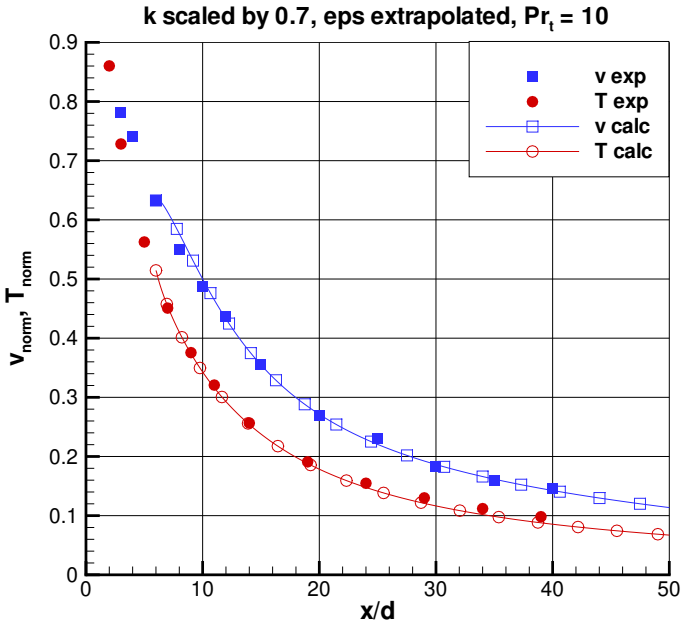

Figure 10: velocity and temperature axial profiles for case B2.

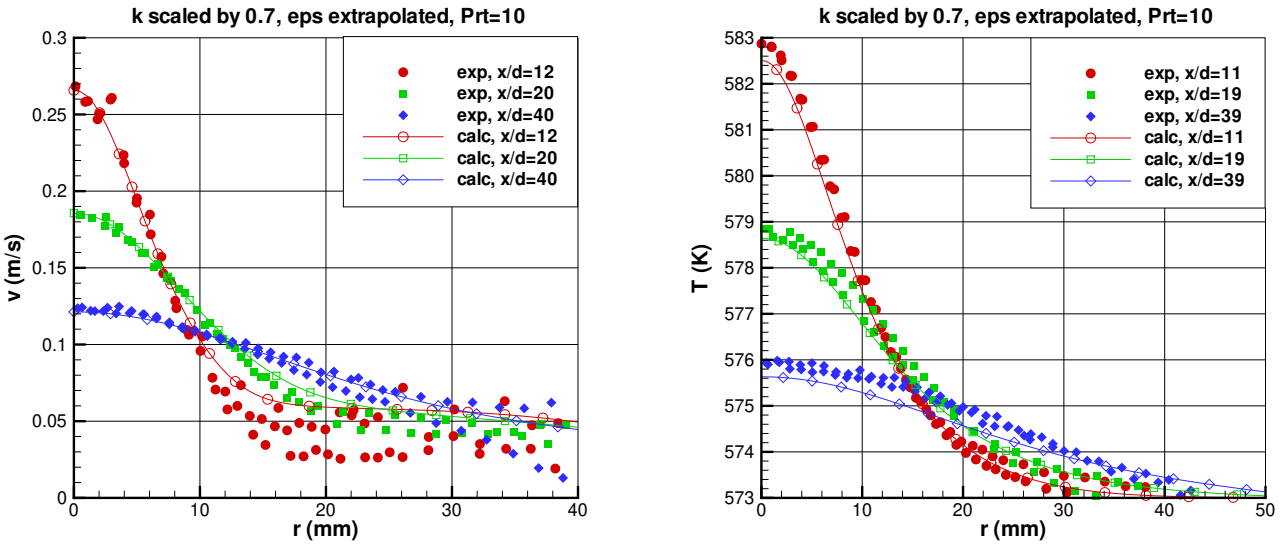

Figure 11: velocity and temperature radial profiles for cases B2.

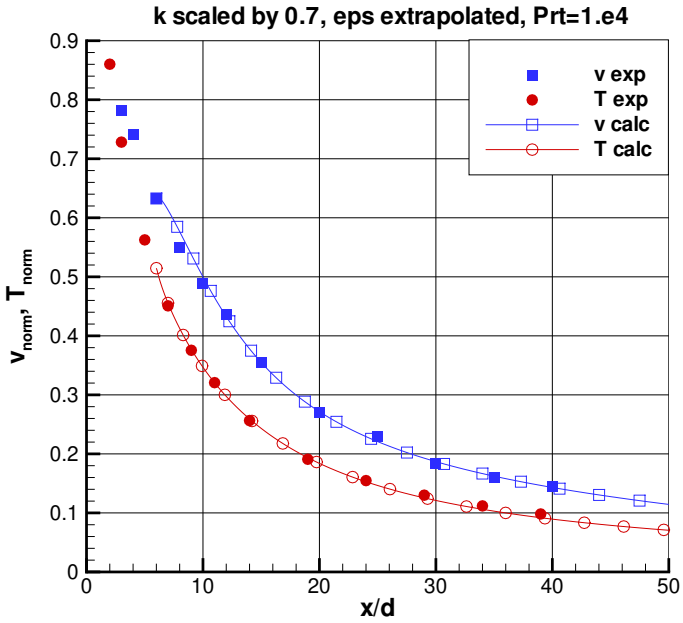

Figure 12: velocity and temperature axial profiles for case B3

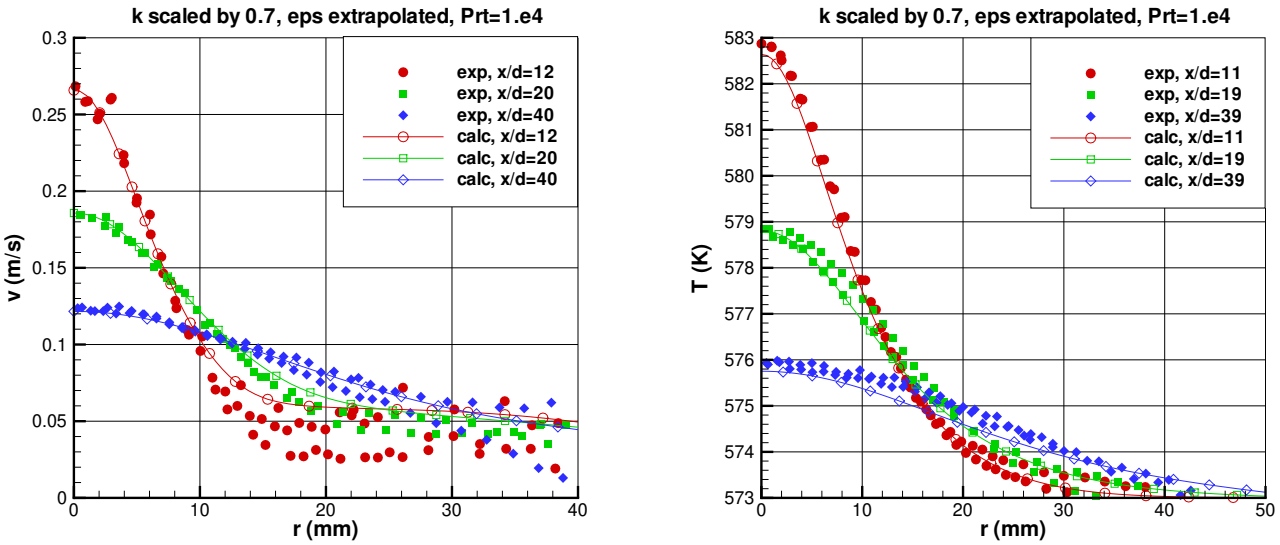

Figure 13: velocity and temperature axial profiles for case B3.

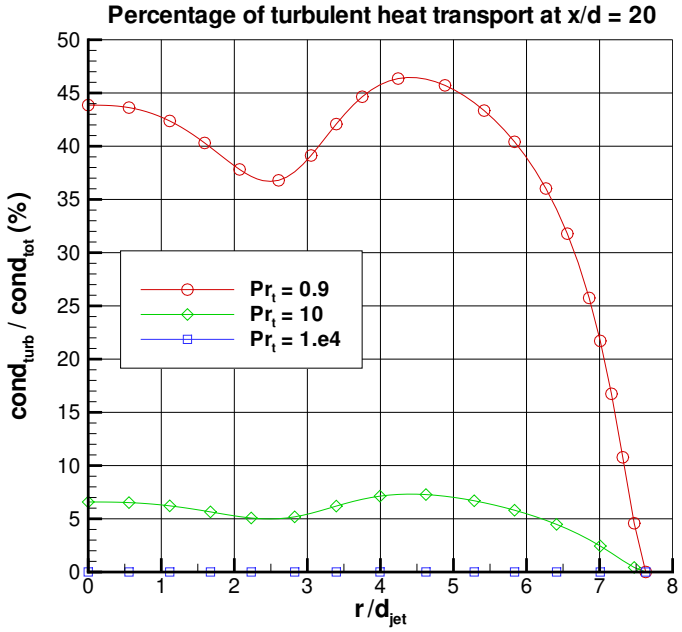

Figure 14: percentage of turbulent heat transport at x/d = 20 for cases B1, B2 and B3.

5 Conclusions

The results of the simulation of the forced-flow case of the TEFLU benchmark, obtained at CRS4 with the Star-CD code, have been reported.

Different versions of the k-ε model implemented in Star-CD have been tested. A precise answer about the capability of such models at simulating the correct jet velocity field cannot be deduced, due to the uncertainties in the inlet turbulence boundary conditions. However, the Chen k-ε showed the lowest tendency to over-predict the jet spreading-rate.

A comparison between the calculated molecular and turbulent heat transport coefficients (calculated with the standard value $Pr_t = 0.9$) showed that they were of the same order of magnitude. In these conditions, a turbulent Prandtl number of order 1 yields an overestimation of the turbulent heat transport.

Some calculations were performed with the inlet k profile scaled in order to fit experimental velocity profiles; then, different values of Pr_t were tested. Good results were found using $Pr_t=10$, calculated with the relation from Jisha and Rieke [6] However, the best results were found with $Pr_t=10^4$, leading to the conclusion that the main heat transport mechanism in the forced-flow case of the TEFLU benchmark is molecular conduction.

From the above results, nothing can be said about the validity of the Reynolds analogy for this kind of flow. However, even in the case it can be applied, a turbulent Prandtl number of order 1 is unsuitable for low-Reynolds-number flows of low-Prandtl-number fluids.

6 References

[1] L. Maciocco, "Proposal for the benchmarking activity on the TEFLU sodium jet experiment", CRS4 Internal Note 00/05

[2]J. U. Knebel et al., "Experimental investigation of a confined heated sodium jet in a co-flow", *J. Fluid Mech. (1998), vol. 368, pp. 51-79.*

[3] S. Corrsin, "Investigation of flow in an axially symmetric heated jet of air", *NACA wartime report, W-94, 1943.*

[4] "Star-CD v3.05 User Manual", *Computational Dynamics Limited, 1998.*

[5] Y.S. Chen, S.W. Kim, *"Computation of turbulent flows using an extended k-ε turbulence closure model*", NASA CR-179204, 1996

[6] M. Jisha, H.B. Rieke, "Modeling assumptions for turbulent heat transfer"

[7] "FLUENT 5 User's Guide Volume 2", *FLUENT Incorporated, 1998.*

[8] D. C. Wilcox, "Turbulence Modeling for CFD", *DCW Industries, Inc., 1994.*

[9] L. Maciocco, M. Mulas, "Analysis of Star-CD Numerical Performances", *CRS4 Internal Note 5-97, 1997.*